https://doi.org/10.5194/egusphere-2024-4041
Preprint. Discussion started: 14 January 2025

How COVID-19 related policies reshaped organic aerosol source contributions in central London

Gang I. Chen[1]*, Anja H. Tremper[1], Max Priestman[1], Anna Font[2], and David C. Green[1,3]

[1]MRC Centre for Environment and Health, Environmental Research Group, Imperial College London, 86 Wood Lane, London, W12 0BZ, UK

[2]IMT Nord Europe, Europe, Institut Mines-Télécom, Univ. Lille, Centre for Education, Research and Innovation in Energy Environment (CERI EE), 59000 Lille, France

[3]HPRU in Environmental Exposures and Health, Imperial College London, 86 Wood Lane, London, W12 0BZ, UK

*Correspondence to: Gang I. Chen (gang.chen@imperial.ac.uk)

https://doi.org/10.5194/egusphere-2024-4041
Preprint. Discussion started: 14 January 2025

Abstract

Particulate matter (PM) poses both health and climate risks. Understanding pollution sources is therefore crucial for effective mitigation. Positive Matrix Factorization (PMF) of Aerosol Chemical Speciation Monitor (ACSM) data is a powerful tool to quantify organic aerosol (OA) sources. A year-long study of ACSM data from London's Marylebone Road monitoring station during the COVID-19 pandemic provides insights into the impact of lockdown and the Eat Out To Help Out (EOTHO) scheme, which offered support to the hospitality during the pandemic, on PM composition and OA sources. Five OA sources were identified including hydrocarbon-like OA (HOA, traffic-related, 11% to OA), cooking OA (COA, 20%), biomass burning OA (BBOA, 12%), more-oxidized oxygenated OA (MO-OOA, 38%), and less-oxidized oxygenated OA (LO-OOA, 21%). Lockdown significantly reduced HOA (-52%), COA (-67%), and BBOA (-41%) compared to their pre-COVID levels, while EOTHO increased COA (+38%) significantly compared to the post-lockdown period. However, MO-OOA and LO-OOA were less affected, as these primarily originated from long-range transport. This research has highlighted the importance of commercial cooking as a significant source of OA (20%) and PM_1 (9%) in urban areas. The co-emission of BBOA with COA observed in Central London demonstrates a similar diurnal cycle and response to the EOTHO policy, indicating that cooking activities might be currently underestimated and contribute to urban BBOA. Therefore, more effort is required to quantify this source and develop targeted abatement policies to mitigate emissions as currently limited regulation is in force.

https://doi.org/10.5194/egusphere-2024-4041
Preprint. Discussion started: 14 January 2025

1 Introduction

Atmospheric particulate matter (PM) are tiny particles suspended in the air, which can not only impact the climate directly and indirectly (IPCC, 2021; Seinfeld et al., 2006), but also cause adverse health effects to human (Kelly and Fussell, 2012; World Health Organization, 2021). PM consist of various constituents, including inorganic species (metals, minerals, black carbon, nitrate, sulphate, etc.) and organic species (complex mixture of thousands of compounds). European Environment Agency has reported that 99% of urban population in Europe are still exposed to polluted air with annual $PM_{2.5}$ (PM with aerodynamic diameter smaller than 2.5 μm) concentrations exceeding the WHO air quality guideline, 5 $\mu g/m^3$ (Europe's air quality status 2024, 2024; World Health Organization, 2021). As the most health-relevant air pollutant, $PM_{2.5}$ has shown strong associations with cardiovascular and respiratory related mortalities and hospital admissions (Dominici et al., 2006; Wei et al., 2022, 2024). Several studies have demonstrated that different constituents/sources contribute to health effects differently with varying toxicities (Kelly and Fussell, 2012). Therefore, targeting the specific composition/sources of PM that are most health-relevant could be the most cost-effective way to mitigate its adverse health effects.

Source apportionment is a common but powerful approach to identifying and quantifying the emission sources and atmospheric constituents of PM based on measurements. As the sources of inorganic species (black carbon, ammonium, nitrate, chloride, sulphate, etc.) are relatively well-studied, most of the studies are focused on deconvoluting the sources of organic aerosol (OA), which contains thousands of compounds. Positive matrix factorization (PMF) is one of the receptor models that is widely utilized in the field to conduct source apportionment analysis. Typically, an Aerodyne aerosol mass spectrometer (AMS, Aerodyne Ltd., USA, Jayne et al., 2000) is used to measure the time series of both inorganic and organic species of non-refractory PM, in which,

https://doi.org/10.5194/egusphere-2024-4041
Preprint. Discussion started: 14 January 2025

organic mass spectra are used for PMF analysis. However, operating an AMS is labour-intense and expensive. In contrast, the aerosol chemical speciation monitor (ACSM, Aerodyne, Ltd., Fröhlich et al., 2013; Ng et al., 2011) has been designed for long-term monitoring purposes with less maintenance and lower capital cost, which has gained popularity across Europe (Chebaicheb et al., 2024; Chen et al., 2022) and the U.S. (https://ascent.research.gatech.edu/). Chen et al. (2022) demonstrated a robust protocol to conduct advanced PMF analysis on long-term ACSM datasets, which delivers high-quality and consistent source apportionment results. This study follows this standardized protocol to resolve the OA sources in London by implementing advanced PMF techniques.

Coronavirus disease 19 (COVID-19) started to spread rapidly worldwide since the first case was identified in Wuhan, China late in 2019. Many countries implemented measures to contain COVID cases, which significantly restricted social and economic activities. In the UK, starting from the end of Mar 26th, 2020, people were ordered to stay at home and all non-essential businesses were closed, including pubs, cafes and restaurants. Non-essential shops were allowed to open on Jun 15th, and the first national lockdown came to an end Jun 23rd, 2020. However, pubs, restaurants, and cafes were only allowed to open from July 4th, 2020. Subsequently, the Eat Out to Help Out (EOTHO) Scheme was designed to help the hospitality industry; offering a 50% meal discount up to a maximum of £10 and operated Monday to Wednesday during from Aug 3rd to Aug 31st, 2020; https://www.gov.uk/guidance/get-a-discount-with-the-eat-out-to-help-out-scheme.

The UK recorded a 2.5% drop in Gross Domestic Product (GDP) in the first quarter of 2020, partly as people reduced their own activity prior to the legally enforced lockdown measures introduced on Mar 26th. This accelerated to a 19.8% fall in GDP in April to June 2020 and household spending fell by over 20% over this period, the largest quarterly contraction on record, which was driven by

https://doi.org/10.5194/egusphere-2024-4041
Preprint. Discussion started: 14 January 2025

falls in spending on restaurants, hotels, transport, and recreation (GDP and events in history: how the COVID-19 pandemic shocked the UK economy, 2024).

Some studies have investigated the lockdown impacts on chemical composition and sources of PM, which mainly focused on cities in China (Hu et al., 2022; Tian et al., 2021; Xu et al., 2020), a kerbside site in Toronto, Canada (Jeong et al., 2022), and an urban background site in Paris, France (Petit et al., 2021). These studies all resolved primary sources including traffic related emissions, biomass burning emissions from residential heating, cooking emissions (except Paris), and secondary sources from PMF analysis on OA. Traffic and cooking emissions appeared to decrease during the lockdown in all sites, while biomass burning predominately from residential heating sources in Chinese cities increased as result of remote work and rather early lockdown measures (Jan-Feb 2020) compared to France. Secondary organic aerosol (SOA) showed a more complex phenomenon given its abundance in organic components and dynamic spatiotemporal conditions. Overall, the lockdowns resulted in decreased SOA in both northwest cities in China (Tian et al., 2021; Xu et al., 2020) and Paris (Petit et al., 2021) due to lower primary emissions, and therefore fewer SOA formation products. However, Beijing experienced a large increase in SOA concentrations due to increased fossil fuel and biomass emissions, long-range transport influences as well as favourable meteorological conditions (high RH, low wind speed and low boundary layer height) for SOA formation during the lockdown period (Hu et al., 2022). Therefore, the lockdown effects on the SOA were dependent on the abundance of primary emissions, long-range transported air masses, and meteorological conditions. To date, there are few studies that investigate how COVID-related policies could have impacted PM chemical composition and sources. Petit et al. (2021) and Gamelas et al., 2023) are only two studies in Europe. The unique COVID-related policies in the UK provided a rare opportunity to investigate the impacts these

https://doi.org/10.5194/egusphere-2024-4041
Preprint. Discussion started: 14 January 2025

policies had on chemical composition and OA sources. To address these issues, we used highly time resolved measurements from an air quality supersite located in the Central London from 2019 to 2020, and advanced source apportionment approaches to quantify the influence of the first lockdown and EOTHO scheme on the PM composition and OA sources. This provides unique insight into PM sources and composition in a global mega city.

2 Methodology

2.1 Air quality monitoring supersite in central London

The London Marylebone Road supersite (MY, 51.52 N, -0.15 E) is a kerbside monitoring site, one meter away from a busy 6-lane road in central London. It is a well-established air quality supersite that has consistently generated high-quality air pollution data since 1997 including mass concentration of bulk PM_1, $PM_{2.5}$, and PM_{10}, as well as PM composition including black carbon, heavy metals, nitrate (NO_3), sulphate (SO_4), ammonium (NH_4), OA, Chloride (Cl), etc. More details of this site can be found at https://uk-air.defra.gov.uk/networks/site-info?site_id=MY1.

2.2 Instrumentations

Quadrupole ACSM (Q-ACSM, Aerodyne, Ltd., Ng et al. (2011)) provides 30-min mass loadings of chemical species within non-refractory submicron aerosol (NR-PM_1), including NH_4, NO_3, SO_4, Cl, and OA. Sampled particles are focused into a narrow beam using the aerodynamic lens and impacted on a filament surface at 600 °C, where the NR-PM_1 is vaporised and ionised instantly by an electron impact source (70eV). These ions are detected by the RGA quadrupole mass spectroscopy to provide a mass spectrum of NR-PM_1 up to a mass-to-charge ratio (*m/z*) of 148 Th. The mass concentration of different chemical species are calculated using the fragmentation table

https://doi.org/10.5194/egusphere-2024-4041
Preprint. Discussion started: 14 January 2025

126 developed by Allan et al. (2004), updated for Cl following suggestions provided by Tobler et al.
127 (2020), and a (Canagaratna et al., 2007; Matthew et al., 2008) composition-dependent collection
128 efficiency (CDCE) correction suggested by Middlebrook et al. (2012) by following the ACTRIS
129 standard operation procedure (https://www.actris-ecac.eu/pmc-non-refractory-organics-and-
130 inorganics). With co-located black carbon (BC) measurement using a $PM_{2.5}$ cyclone with AE33
131 (Aerosol Magee Scientific, Ltd.) and PM_1 measurements using FIDAS (Palas, GmbH), we
132 conducted the mass closure for fine particles measurements. The sum of NR-PM_1 and BC (in $PM_{2.5}$)
133 reproduces PM_1 concentrations well, with a slope of 1.13 and an R^2 of 0.73 (Fig. S1).

134 ### *2.3 Sampling periods and COVID-related policies*

135 PM_1 chemical composition from Aug 1st, 2019 to Oct 22nd, 2020, was analysed as this covered the
136 first lockdown period (Mar 26th–23 Jun 23rd, 2020) and the EOTHO Scheme (Mon-Wed during
137 from Aug 3rd to Aug 31st, 2020, Table 1). In order to isolate the seasonal effects on the PM chemical
138 composition and OA sources from the COVID-related policies, we further split the data based on
139 seasons (Table 1).
140

https://doi.org/10.5194/egusphere-2024-4041
Preprint. Discussion started: 14 January 2025

Table 1 Dates of the COVID-related policies in London

COVID Policies		Date
Pre-Lockdown	Summer	Aug 1st–Aug 31st, 2019
	Fall	Sep 1st–Nov 30th, 2019
	Winter	Dec 1st, 2019–Feb 28th, 2019
	Spring	Mar 1st–Mar 25th, 2020
Lockdown	Spring	Mar 26th–May 31st, 2020
	Summer	Jun 1st–Jun 23rd, 2020
Post-Lockdown	Pre-EOTHO	Jun 24th–Aug 2nd, 2020
	EOTHO	Aug 3rd–Aug 31st, 2020
	Post-EOTHO	Sep 1st–Oct 22nd, 2020

2.4 Source apportionment

Positive matrix factorization (PMF) has been widely deployed in source apportionment of PM components including OA from ACSM/AMS datasets collected worldwide (Chebaicheb et al., 2024; Chen et al., 2022; Jimenez et al., 2009; Ng et al., 2011b; Zhang et al., 2011). The PMF algorithm on environmental monitoring data was initially introduced by Paatero and Tapper, (1994) as follows:

$$x_{ij} = \sum_{k=1}^{p} g_{ik} \times f_{kj} + e_{ij} \quad (1)$$

where x_{ij} is the measurement matrix (here, the time series of organic mass spectra from the ACSM at i^{th} time and j^{th} *m/z*), g_{ik} is the mass concentration at i^{th} *time* in k^{th} factor, f_{kj} is the relative

https://doi.org/10.5194/egusphere-2024-4041
Preprint. Discussion started: 14 January 2025

intensity of j^{th} *m/z* for k^{th} factor, and e_{ij} stands for the residuals for j^{th} *m/z* at i^{th} time, *p* is the number of factors. The PMF model iteratively minimises the *Q* value using the least-squares algorithm as:

$$Q = \sum_{i=1}^{n}\sum_{j=1}^{m}\left(\frac{e_{ij}}{\sigma_{ij}}\right)^2 \quad (2)$$

where *n* is the number of data points, *m* is the total number of *m/z*, and σ_{ij} is the measurement uncertainty estimated before the PMF analysis at i^{th} time for j^{th} *m/z*.

However, PMF suffers from rotational ambiguity (Paatero et al., 2002), which provides non-unique solutions (i.e., similar Q value with different time series and factor profiles). These solutions typically will not be equally environmentally reasonable, even with similar Q values. The multilinear engine ME-2 (Paatero, 1999; Paatero and Hopke, 2009) is a robust approach to reduce the rotational ambiguity and can direct PMF towards environmentally reasonable solutions (both factor profiles and time series).

Here, PMF was implemented using the Source Finder v9.5.1.3 (Datalystica Ltd., Switzerland, Canonaco et al. 2013) with the ME-2 solver. The latter imposes *a priori* information on the factor solutions and/or time series. The *a*-value (ranging from 0 to 1) represents the upper limit of the relative deviation for a factor profile (f_j) or time series (g_i) from the chosen *a priori* input profile (F_j) or time series (G_i) during the iterative least-square minimization (Equation 2), as shown in Equations 3a and 3b (Canonaco et al., 2013):

$$f_j = F_j \pm a \cdot F_j \quad (3a)$$

$$g_i = G_i \pm a \cdot G_i \quad (3b)$$

https://doi.org/10.5194/egusphere-2024-4041
Preprint. Discussion started: 14 January 2025

PMF analysis is usually performed using the whole dataset, assuming that the OA source profiles are static over the entire period, which can lead to high errors when it comes to long-term datasets with non-negligible temporal variabilities of OA chemical fingerprints. Canonaco et al. (2015) showed a considerable seasonal variability of oxygenated organic aerosol (OOA) factor profiles, especially between winter and summer in a dataset in Switzerland. Parworth et al. (2015) first introduced the concept of rolling PMF by shortening the analysis period to a smaller time window (e.g., 14 days) and then rolling over the whole dataset with a certain step (i.e., 1 day). This technique was further refined and implemented into SoFi by Canonaco et al. (2021), which allows the PMF model to adapt the temporal variabilities of the source profiles (e.g., biogenic versus biomass burning influences on OOA factors), which usually provides well-separated OA factors.

Bootstrapping (Efron, 1979) analysis will randomly select part of the PMF input matrix and duplicates itself to recreate a matrix with the same dimension as the original PMF input matrix. The statistical and rotational uncertainties of the PMF results will then be evaluated by bootstrap and the random *a*-value approach with at least 50 repeats per rolling window (Canonaco et al., 2021; Chen et al., 2021). The standardized protocol of rolling PMF as presented in Chen et al. (2022) was used to ensure high-quality and comparable sources of OA were retrieved in London.

Specifically, PMF was first done on four different seasons as suggested in Chen et al. (2022) to determine the optimum number of factors. A total of 5 OA factors were identified: hydrocarbon-like OA (HOA), cooking-like OA (COA), biomass burning OA (BBOA), more-oxidized OOA (MO-OOA) and less-oxidized OOA (LO-OOA). In addition, site-specific factor profiles were derived for HOA, COA, and BBOA through a seasonal bootstrap PMF analysis for winter (Dec, Jan, and Feb) and used as constraints as suggested in Chen et al. (2022) and Via et al. (2022). However, the MY site is surrounded by many restaurants with prevalent cooking emissions. Thus,

https://doi.org/10.5194/egusphere-2024-4041
Preprint. Discussion started: 14 January 2025

the chemical fingerprint for both HOA and COA might not be fully separated. Therefore, we constrained the trend of NO_x time series, BBOA and COA profiles from a previous winter bootstrap solution collected in London North Kensington (2015-2018, Chen et al., 2022) to retrieve environmentally reasonable results with five factors, so-called base case solution. Then, a bootstrap resampling analysis with 100 iterations and five factors was conducted by constraining the factor profiles of HOA, COA, and BBOA from the base case with random a-value from 0.1-0.5 with step of 0.1. It results in stable factor profiles of these three primary sources as shown in Figure S2, which shows good agreements with published reference profiles (Chen et al., 2022; Crippa et al., 2013).

By constraining primary factor profiles of HOA, COA, BBOA in Figure S2 (averaged bootstrap results) and two additional unconstrained factors with bootstrap resampling and the random a-value option (0.1-0.5, step of 0.1), rolling PMF is conducted with a time window of 14 days and a step of 1 day. A criteria list including selections based on both time series and factor profiles as shown in Table S1 was applied as per Chen et al. (2022). With the help of t-test in temporal-based criteria (1-3), we can minimize subjective judgements in determining the environmentally reasonable results. Eventually, 3,166 runs (14.1%) of the PMF runs were selected to average as the final results with 4.9 % unmodelled data points, which is comparable with other rolling PMF analyses (Chen et al., 2022).

https://doi.org/10.5194/egusphere-2024-4041
Preprint. Discussion started: 14 January 2025

3 Results and Discussions

3.1 Chemical composition of submicron PM for different periods around the COVID-19 Lockdown

The average PM_1 mass concentration at MY site was 11 µg/m^3 for the study period with 44% OA, 21% NO_3, 15% SO_4, 16% BC, 5% NH_4, and 0.6% Cl. The distribution of the chemical composition on PM_1 varied depending on the season and variation was associated with the lockdown and EOTHO policies (Figure 1). PM_1 increased by 34% in lockdown spring (Mar 26th–May 31st, 2020) compared to pre-lockdown spring (Mar 1st–Mar 25th, 2020), as well as NO_3 and NH_4, the later most likely originated from enhanced agricultural emissions in spring from the UK and wider continental Europe (Aksoyoglu et al., 2020). It was further confirmed, through back trajectory analysis, that elevated PM_1 events (Mar 25th–Mar 28th, Apr 8th–Apr 10th, and Apr 15th–Apr 17th), where the result of airmasses passing over northern continental Europe (Figure S3). NO_3 concentration reduced in summer 2019 and 2020 as expected compared to spring or fall seasons due to the volatility of NH_4NO_3, while SO_4 concentrations increased in summer due to enhanced photochemistry. During the lockdown in spring SO_4 concentrations remained high, which was associated with long-range transport.

https://doi.org/10.5194/egusphere-2024-4041
Preprint. Discussion started: 14 January 2025

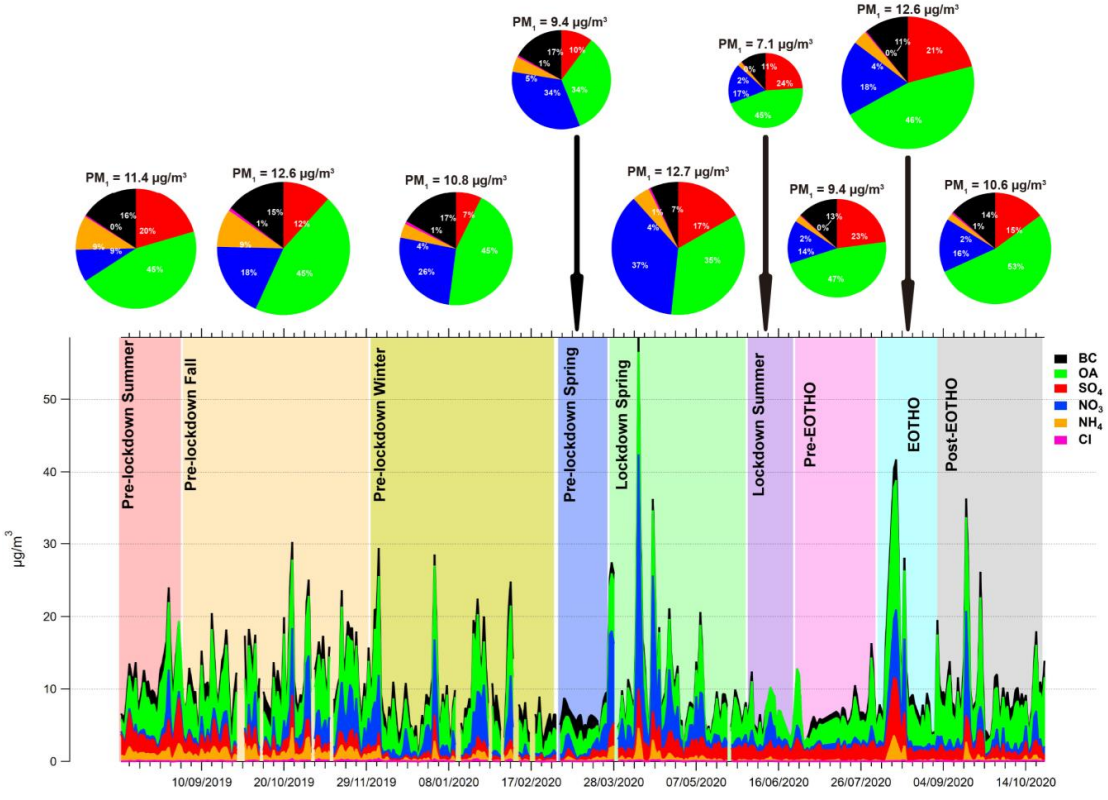

Figure 1 Chemical compositions of PM_1 at MY from Aug 2019 to Oct 2020 (daily resolution) and averaged for the different periods as shown in Table 1.

BC concentrations during the spring lockdown (Mar 26th–May 31st 2020) reduced from 1.59 to 0.87 µg/m^3 (-45%) compared to the pre-lockdown level in spring (Mar 1st–Mar 25th), due to the significant reduction in traffic during the first lockdown (Transport for London, 2020). It is worth noting that the BC concentration had already reduced by 13% in pre-lockdown spring (Mar 1st–Mar 25th) compared to the pre-lockdown winter. This is likely due to vehicle mileage reducing as the UK government implemented travel restrictions and advised people to work from home on Mar 16th, 2020 (Transport for London, 2020). BC increased to 1.24 µg/m^3 (+57%) after the lockdown and before the EOTHO (Jun 24th–Aug 2nd,2020, pre-EOTHO in Figure 1) as people returned to work and travel. However, BC concentrations remained 31% lower than the pre-

https://doi.org/10.5194/egusphere-2024-4041
Preprint. Discussion started: 14 January 2025

lockdown summer (Aug 1st–Aug 31st, 2019) concentration of 1.8 μg/m^3, which suggests that the traffic emissions reduced considerably as the fewer economic activities even after the ease of the first lockdown (e.g., suggestions of hybrid working mode, restricted international travel, reduced tourism, limited access to entertainments). BC also increased to 1.4 μg/m^3 (+10%) during the EOTHO scheme (Aug 3rd–Aug 31st, 2020). This was not only because of increased traffic emission during this period, but may also result from cooking activities (e,g, barbecuing or wood-fired cooking styles) in central London. BC concentrations increased on Mon-Tue compared to post-lockdown but before EOTHO (Jun 24th–Aug 2nd, 2020) (Figure S4).

3.2 OA sources in Central London

As mentioned above, the rolling PMF analysis resolved 5 factor solutions, including HOA, COA, BBOA, MO-OOA, and LO-OOA as shown in Figure 2 and Figure 3. The left panel of Figure 2 shows the yearly averaged factor profiles of resolved PMF factors and total OOA calculated as the sum of LO-OOA and MO-OOA. All factors show good agreements with previous studies in terms of key *m/z*.

3.2.1 Time series of OA factors

Figure 2 shows both time series (30-min time resolution) and diurnal cycles for each OA factor. The mean concentrations of HOA, COA, BBOA, MO-OOA, LO-OOA, and OOA were 0.50 ± 0.1 μg/m^3, 0.93 ± 0.14 μg/m^3, 0.55 ± 0.11 μg/m^3, 1.81 ± 0.41 μg/m^3, 1.00 ± 0.44 μg/m^3, and 2.80 ± 0.70 μg/m^3, respectively, and contributed to OA (PM_1) with the fractions of 11% (5% to PM_1), 20% (9% to PM_1), 12% (5% to PM_1), 38% (17% to PM_1), 21% (9% to PM_1), and 59% (26% to PM_1). The concentration of all OA factors shows strong time variations over the year as shown on the left panel of the Figure 2. OA factors also showed strong seasonality besides the effects from

https://doi.org/10.5194/egusphere-2024-4041
Preprint. Discussion started: 14 January 2025

257 COVID-related policies (Figure 3). POA concentrations were generally lower in the warmer
258 seasons than in winter as lower temperature favours particle formation via condensation and
259 dilution and dispersion are reduced due to the lower boundary layer. The OOA factor
260 concentrations were larger the warmer seasons due to enhanced photochemistry at higher
261 temperature, stronger solar radiation and increased VOC emissions. The seasonality observed here
262 in central London agreed with the other sites across Europe (Chen et al., 2022).

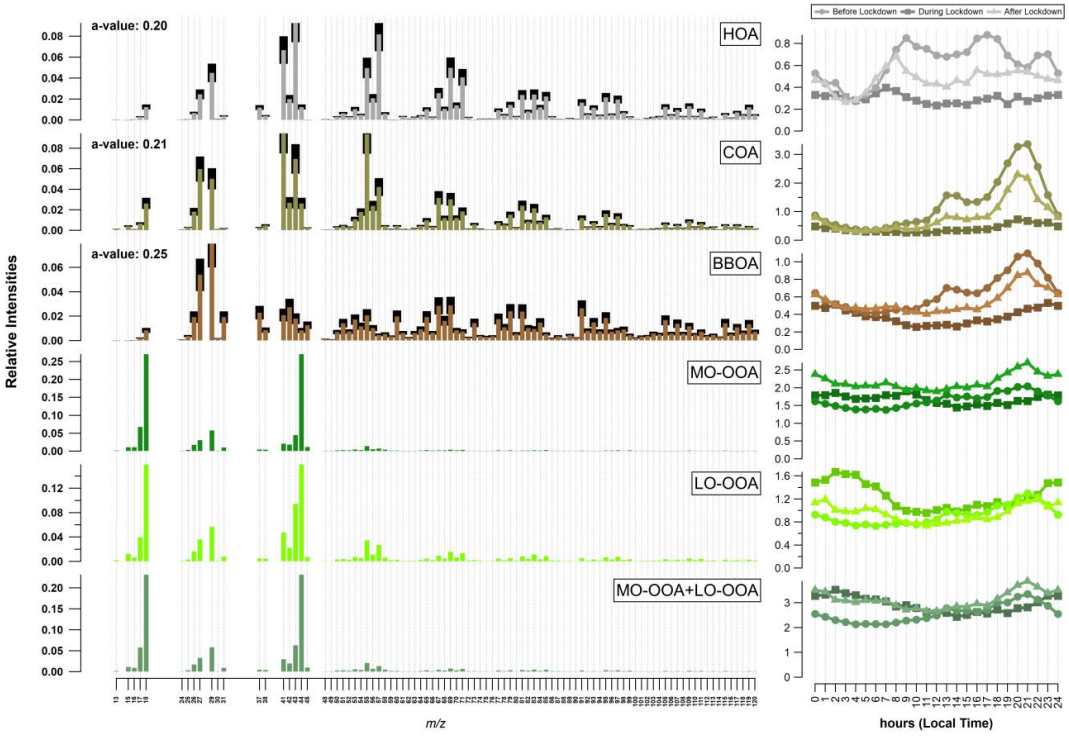

263

264 *Figure 2 Yearly averaged profiles (left) and diurnal cycles (right) of resolved factors from the rolling PMF analysis at the MY site.*
265 *Time is expressed in local time.*

266 ### 3.2.2 Diurnal Cycles for OA factors

267 The right side of Figure 2 shows the diurnal cycles before, during, and after the lockdown. POA
268 factors showed distinct diurnal variations, in which HOA showed morning and evening rush hour
269 peaks, COA showed distinct lunchtime and evening peaks, and BBOA showed a similar pattern

https://doi.org/10.5194/egusphere-2024-4041
Preprint. Discussion started: 14 January 2025

as COA before and after the lockdown. This indicates that the part of what is measured as BBOA in central London is most likely co-emitted from cooking activity, most likely from barbecuing style restaurants in the area. Mohr et al. (2009) showed that meat-cooking can slightly elevate *m/z* 60, which is an important ion in the BBOA factor profile. OOA factors showed much less diurnal variation compared to POA factors in all periods, this is in agreement with the other 22 European sites reported in Chen et al. (2022). The MO-OOA showed a smaller diurnal variation compared to LO-OOA.

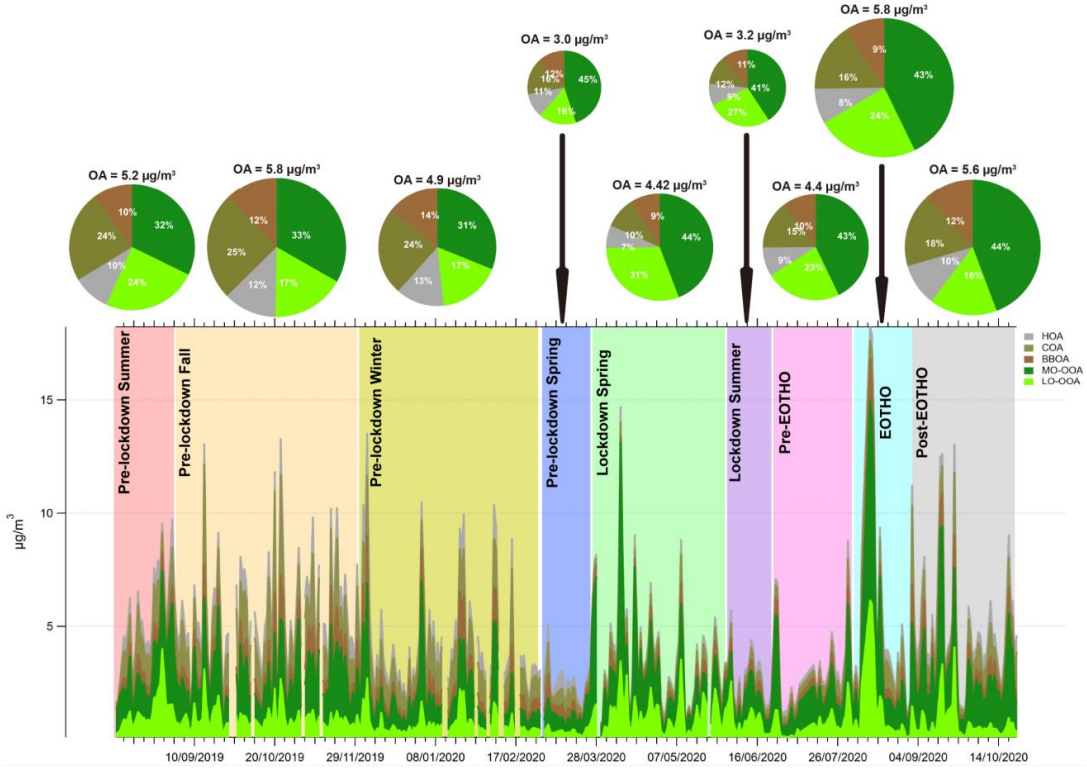

Figure 3 Average mass concentrations for OA sources at MY during different periods from Aug 2019 to Oct 2020

The diurnal variation of COA and BBOA during lockdown lost the distinctive lunch peak as shown in the pre-lockdown; and the evening peak reduced its intensity (Figure 2). HOA retained distinct morning and evening rush hour peaks but at lower mass concentrations during lockdown (Figure

https://doi.org/10.5194/egusphere-2024-4041
Preprint. Discussion started: 14 January 2025

282 2). After the first lockdown, the distinct lunch and evening peaks in diurnal patterns of COA and
283 BBOA reappeared as the open-up of nearby restaurants. The morning and evening rush hour peaks
284 for HOA enhanced considerably as the ease of the travel restrictions after the first lockdown.
285 However, POA concentrations did not reach pre-COVID levels. This is likely due to widespread
286 hybrid working and the remaining oversea travel restrictions supressing tourism, which reduced
287 traffic activity and restaurants visits. Conversely, OOA concentrations were slightly higher than
288 pre-lockdown levels. These were related to long-range transport, with relatively high mass
289 concentrations of MO-OOA and LO-OOA during the lockdown (Figure S3).

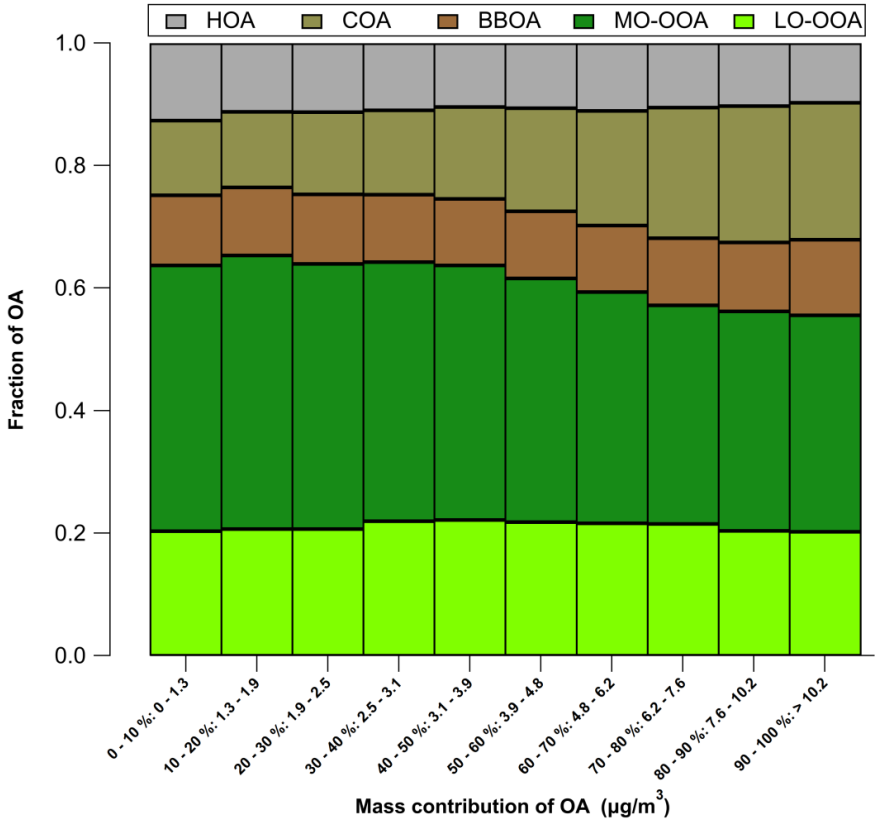

290

291 *Figure 4 Contributions to total OA from the different identified OA sources at different OA concentrations. Total OA*
292 *concentrations were split in 10 equally distributed bins.*

https://doi.org/10.5194/egusphere-2024-4041
Preprint. Discussion started: 14 January 2025

As shown in Figure *4* The contribution to total OA concentrations from HOA, BBOA, and LO-OOA was consistent at different OA concentrations. However, the contribution of COA increased as total OA concentrations increased (Figure *4*), This suggests that cooking emissions in Central London are responsible for elevated OA concentrations.

3.2.3 Impact of lockdown on OA Concentrations

OA concentration decreased by 34% in pre-lockdown spring compared to pre-lockdown winter (Dec 1st, 2019–Feb 28th, 2020) due to seasonality and the impact of lockdown. OOA concentrations were relatively unaffected with some variability before, during, and after the lockdown. due to long-range transportation of airmasses from the continental Europe as observed for NH_4, NO_3, and SO_4. Primary emissions were significantly lower due to reduced vehicle mileage and other economic activity before the official lockdown measure came into force (Figure 3 and Figure 2 (a)) as suggested by the 1st quarter drop in GDP. Atmospheric components related to vehicles (HOA and BC) decreased by 50% and 13% respectively, in early March 2020. COA and BBOA decreased by 60% and 47% respectively. COA, due to fewer restaurant activity, BBOA likely reduced partly due to the warmer weather requiring less domestic space heating, and also due to reduced commercial cooking using charcoal and wood.

Compared to the pre-lockdown spring, HOA and COA in the lockdown spring decreased by 8% and 11%, respectively, while BBOA increased marginally by 5% (from 0.37 to 0.39 $\mu g/m^3$) (Figure 3). MO-OOA and LO-OOA increased by 43% and 169%, respectively due to long-range transportation of airmasses from continental Europe and increased photochemistry compared to the first 25 days in Mar 2020. This was accompanied by increased SO_4 (+119%), NH_4 (+16%) and

https://doi.org/10.5194/egusphere-2024-4041
Preprint. Discussion started: 14 January 2025

NO_3 (+46%), despite the higher temperature could favour partitioning these species into the gas phase.

In June 2020, still in lockdown (Jun 1st– Jun 23rd, 2020), POA showed further but marginal decreases (-4%, -8%, and -10% for HOA, COA, and BBOA, respectively, Figure 3) compared to the lockdown spring as the enhanced photochemistry leads to increased formation of OOA from the POA. However, the overall mass concentration of MO-OOA and LO-OOA decreased significantly by 34%, and 37%, respectively as the result of fewer long-range transported airmasses. During pre-EOTHO (Jun 24th–Aug 2nd, 2020), HOA, COA, and BBOA all showed considerably increases of 34%, 69%, and 25%, respectively when compared to lockdown summer period. In which, MO-OOA and LO-OOA also increased by 45% and 18%, respectively as the results of long-range transported airmasses from continental Europe, enhanced biogenic emissions and photochemistry. The POA concentrations were much lower when compared to summer 2019 (Aug 1st–Aug 31st, 2019) as travel and economic activities did not return to pre-COVID levels. Specifically, reduced vehicle mileage resulted in lower HOA (-22%), BC (-31%), COA (-46%) due to the reduced commercial cooking activity. As BBOA is co-emitted with COA during of cooking activities, BBOA also decreased slightly from 0.53 to 0.44 μg/m^3 (-17%, Figure 3).

3.2.4 Eat out to help out (EOTHO)

During EOTHO (Aug 3rd–Aug 31st, 2020), MO-OOA and LO-OOA increased by 31% and 35% respectively compared to post-lockdown concentrations before EOTHO and correlated with increased NO_3 and SO_4 concentrations. This was due to long-ranged transported airmasses and enhanced photochemistry as well as the photooxidation of POAs.

https://doi.org/10.5194/egusphere-2024-4041
Preprint. Discussion started: 14 January 2025

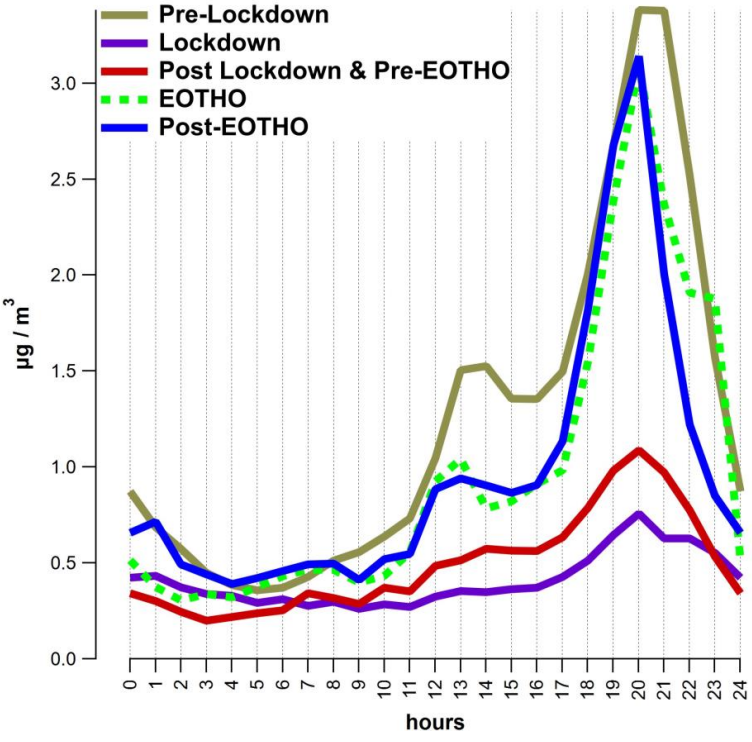

Figure 5 . COA diurnal plots at different periods in relation with COVID-related policies

However, EOTHO policy had a significant impact on all POA factors. In particular, the COA concentration increased by 38% compared to the post-lockdown period from Jun 24th to Aug 2nd, 2020 (Figure 5). HOA and BBOA concentrations also increased by 22% and 23%, respectively, which suggested the human activities resulting in these emissions recovered slowly after the lockdown. COA was significantly higher due to EOTHO, however, it did not reach pre-COVID concentrations (Figure 5). After the EOTHO policy (Sep 1st–Oct 22nd, 2020), COA concentrations increased by 10% (Figure 5). This may have partially been due to lower temperatures, reduced dispersion and photochemistry in Autumn.

EOTHO only operated from Mon to Wed, and this was clear in the diurnal plots (Figure 6) and Figure S6 with larger COA concentrations Mon to Wed, in contrast with larger concentrations over the weekend (Fri to Sun) before EOTHO (Jun 24th–Aug 2nd, 2020). Interestingly, even after the

https://doi.org/10.5194/egusphere-2024-4041
Preprint. Discussion started: 14 January 2025

EOTHO policy ceased, COA levels remained elevated on Mon and Tue but a much higher level during the weekend was observed. This suggests that EOTHO had an influence on the consumer behaviour even after the lockdown. It is also worth noting that the high concentrations of COA and BBOA (Figure S5) on Monday night were caused by the last day of EOTHO policy coinciding with a UK public holiday on Aug 31st.

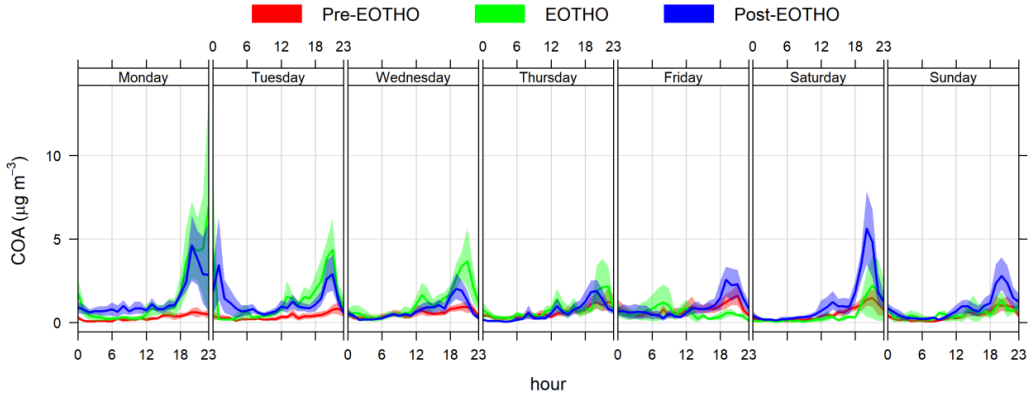

Figure 6 The diurnal cycles for each day of the week in COA concentrations before, during, and after the Eat Out To Help Out (EOTHO) policy in post-lockdown period (Jun 24th–Oct 22nd, 2020)

4 Conclusion

This study demonstrates the importance of source apportionment studies to better understand how national and local government policies can impact the PM mixture, and how these effects can be differentiated from the influences of meteorology and large-scale atmospheric processes. PM concentrations increased at the beginning of the lockdown (Mar–Apr 2020), coinciding with reduced economic activities, however by examining the source apportionment (and inorganic PM composition) the impact of lockdown policies on primary emissions could be quantified. COVID-related policies were found to have profound but largely unintended impacts on air quality. The first lockdown significantly reduced POA sources: including HOA by 52%, COA by 67%, and

https://doi.org/10.5194/egusphere-2024-4041
Preprint. Discussion started: 14 January 2025

365 BBOA by 41%. While all these components reduced dramatically during the lockdown, they only
366 gradually increased again and did not reach pre-COVID levels during the duration of this study.
367 Most significantly, while the Eat Out To Help Out (EOTHO) policy was effective in helping the
368 hospitality industry to recover from economic losses during the lockdown, it had unintended
369 impacts on air quality as cooking emissions increased. Clearly detecting this change confirms the
370 presence of COA (20% to OA) as an important source of OA in London, and other cities, and the
371 importance of commercial cooking as a source. Also of note was the impact that EOTHO had on
372 BBOA concentrations, which increased by 23% while this policy was in place. This establishes a
373 clear link between commercial cooking activity and BBOA measured in cities due to the use of
374 charcoal and wood as cooking fuels, as well as potentially emissions from cooking ingredients.
375 Cooking may therefore be underestimated as a source if COA concentrations are considered in
376 isolation, and BBOA is only associated with other sources of solid fuel burning. This emphasises
377 the need to develop policies and technical solutions to mitigate commercial cooking emissions in
378 the urban environment, especially as there are limited regulations on this industry in terms of air
379 pollution. It also demonstrated the importance in continuous monitoring with subsequent source
380 apportionment analysis to better understand the influence of government policies to improve air
381 quality more effectively.

382

https://doi.org/10.5194/egusphere-2024-4041
Preprint. Discussion started: 14 January 2025

Code/Data availability

Rolling PMF analyses is run using SoFi Pro from Datalystica (https://datalystica.com/sofi-pro/, Datalystica, 2024) under Igor Pro 9 platform from WaveMetrics® (https://www.wavemetrics.com/, WaveMetrics, 2024) and they are both available for purchase. Raw data/results from the study are available upon request to the corresponding author Gang I. Chen (gang.chen@imperial.ac.uk).

Author contribution

Gang I. Chen: Writing – review & editing, Writing – original draft, Visualization, Validation, Project administration, Methodology, Investigation, Funding acquisition, Formal analysis, Data curation, Conceptualization. **Anja H. Tremper:** Writing – review & editing, Methodology, Formal analysis, Data curation. **Max Priestman:** Methodology, Formal analysis, Data curation. **Anna Font:** Writing – review & editing, Methodology, Formal analysis, Data curation. **David C. Green:** Writing – review & editing, Supervision, Project administration, Methodology, Resources, Funding acquisition, Conceptualization.

Competing interests

The authors declare that they have no known competing financial interests or personal relationships that could have appeared to influence the work reported in this paper.

Acknowledgement

This study is part funded by the National Institute for Health Research (NIHR) Health Protection Research Unit in Environmental Exposures and Health, a partnership between UK Health Security

https://doi.org/10.5194/egusphere-2024-4041
Preprint. Discussion started: 14 January 2025

Agency (UKHSA) and Imperial College London. The views expressed are those of the authors and not necessarily those of the NIHR, UKHSA or the Department of Health and Social Care. This study was also supported by NERC Awards (NE/1007806/1) and (NE/T001909/2).

References

Aksoyoglu, S., Jiang, J., Ciarelli, G., Baltensperger, U., and Prévôt, A. S. H.: Role of ammonia in European air quality with changing land and ship emissions between 1990 and 2030, Atmos Chem Phys, 20, 15665–15680, https://doi.org/10.5194/acp-20-15665-2020, 2020.

Allan, J. D., Delia, A. E., Coe, H., Bower, K. N., Alfarra, M. R., Jimenez, J. L., Middlebrook, A. M., Drewnick, F., Onasch, T. B., Canagaratna, M. R., Jayne, J. T., and Worsnop, D. R.: A generalised method for the extraction of chemically resolved mass spectra from Aerodyne aerosol mass spectrometer data, J Aerosol Sci, 35, 909–922, https://doi.org/10.1016/j.jaerosci.2004.02.007, 2004.

Canonaco, F., Crippa, M., Slowik, J. G., Baltensperger, U., and Prévôt, A. S. H.: SoFi, an IGOR-based interface for the efficient use of the generalized multilinear engine (ME-2) for the source apportionment: ME-2 application to aerosol mass spectrometer data, Atmos Meas Tech, 6, 3649–3661, https://doi.org/10.5194/amt-6-3649-2013, 2013.

Canonaco, F., Slowik, J. G., Baltensperger, U., and Prévôt, A. S. H.: Seasonal differences in oxygenated organic aerosol composition: implications for emissions sources and factor analysis, Atmos. Chem. Phys., 15, 6993–7002, https://doi.org/10.5194/acp-15-6993-2015, 2015.

https://doi.org/10.5194/egusphere-2024-4041
Preprint. Discussion started: 14 January 2025

424 Canonaco, F., Tobler, A., Chen, G., Sosedova, Y., Slowik, J. G. G., Bozzetti, C., Daellenbach,
425 K. R., El Haddad, I., Crippa, M., Huang, R.-J., Furger, M., Baltensperger, U., Prévôt, A. S.
426 H., Kaspar Rudolf Haddad, I. E. D., Crippa, M., Huang, R.-J., Furger, M., Baltensperger, U.,
427 Prevot, A. S. H., Daellenbach, Kaspar Rudolf Haddad, I. El, Crippa, M., Huang, R.-J., Furger,
428 M., Baltensperger, U., and Prevot, A. S. H.: A new method for long-term source
429 apportionment with time-dependent factor profiles and uncertainty assessment using SoFi Pro:
430 application to 1 year of organic aerosol data, Atmos Meas Tech, 14, 923–943,
431 https://doi.org/10.5194/amt-14-923-2021, 2021.
432 Chebaicheb, H., de Brito, J. F., Amodeo, T., Couvidat, F., Petit, J.-E., Tison, E., Abbou, G.,
433 Baudic, A., Chatain, M., Chazeau, B., Marchand, N., Falhun, R., Francony, F., Ratier, C.,
434 Grenier, D., Vidaud, R., Zhang, S., Gille, G., Meunier, L., Marchand, C., Riffault, V., and
435 Favez, O.: Multiyear high-temporal-resolution measurements of submicron aerosols at 13
436 French urban sites: data processing and chemical composition, Earth Syst Sci Data, 16, 5089–
437 5109, https://doi.org/10.5194/essd-16-5089-2024, 2024.
438 Chen, G., Sosedova, Y., Canonaco, F., Fröhlich, R., Tobler, A., Vlachou, A., Daellenbach, K.
439 R., Bozzetti, C., Hueglin, C., Graf, P., Baltensperger, U., Slowik, J. G., El Haddad, I., and
440 Prévôt, A. S. H.: Time-dependent source apportionment of submicron organic aerosol for a
441 rural site in an alpine valley using a rolling positive matrix factorisation (PMF) window,
442 Atmos Chem Phys, 21, https://doi.org/10.5194/acp-21-15081-2021, 2021.
443 Chen, G., Canonaco, F., Tobler, A., Aas, W., Alastuey, A., Allan, J., Atabakhsh, S., Aurela,
444 M., Baltensperger, U., Bougiatioti, A., De Brito, J. F., Ceburnis, D., Chazeau, B., Chebaicheb,
445 H., Daellenbach, K. R., Ehn, M., El Haddad, I., Eleftheriadis, K., Favez, O., Flentje, H., Font,
446 A., Fossum, K., Freney, E., Gini, M., Green, D. C., Heikkinen, L., Herrmann, H., Kalogridis,

https://doi.org/10.5194/egusphere-2024-4041
Preprint. Discussion started: 14 January 2025

447 A.-C., Keernik, H., Lhotka, R., Lin, C., Lunder, C., Maasikmets, M., Manousakas, M. I.,
448 Marchand, N., Marin, C., Marmureanu, L., Mihalopoulos, N., Močnik, G., Nęcki, J., O'Dowd,
449 C., Ovadnevaite, J., Peter, T., Petit, J.-E., Pikridas, M., Matthew Platt, S., Pokorná, P., Poulain,
450 L., Priestman, M., Riffault, V., Rinaldi, M., Różański, K., Schwarz, J., Sciare, J., Simon, L.,
451 Skiba, A., Slowik, J. G., Sosedova, Y., Stavroulas, I., Styszko, K., Teinemaa, E., Timonen,
452 H., Tremper, A., Vasilescu, J., Via, M., Vodička, P., Wiedensohler, A., Zografou, O., Cruz
453 Minguillón, M., and Prévôt, A. S. H.: European aerosol phenomenology − 8: Harmonised
454 source apportionment of organic aerosol using 22 Year-long ACSM/AMS datasets, Environ
455 Int, 166, 107325, https://doi.org/10.1016/j.envint.2022.107325, 2022.
456 Crippa, M., DeCarlo, P. F., Slowik, J. G., Mohr, C., Heringa, M. F., Chirico, R., Poulain, L.,
457 Freutel, F., Sciare, J., Cozic, J., Di Marco, C. F., Elsasser, M., Nicolas, J. B., Marchand, N.,
458 Abidi, E., Wiedensohler, A., Drewnick, F., Schneider, J., Borrmann, S., Nemitz, E.,
459 Zimmermann, R., Jaffrezo, J.-L., Prévôt, A. S. H., and Baltensperger, U.: Wintertime aerosol
460 chemical composition and source apportionment of the organic fraction in the metropolitan
461 area of Paris, Atmos Chem Phys, 13, 961–981, https://doi.org/10.5194/acp-13-961-2013,
462 2013.
463 Dominici, F., Peng, R. D., Bell, M. L., Pham, L., McDermott, A., Zeger, S. L., and Samet, J.
464 M.: Fine Particulate Air Pollution and Hospital Admission for Cardiovascular and
465 Respiratory Diseases, JAMA, 295, 1127, https://doi.org/10.1001/jama.295.10.1127, 2006.
466 Efron, B.: Bootstrap Methods: Another Look at the Jackknife, The Annals of Statistics, 7, 1–
467 26, 1979.
468 Europe's air quality status 2024:

https://doi.org/10.5194/egusphere-2024-4041
Preprint. Discussion started: 14 January 2025

469 Fröhlich, R., Cubison, M. J., Slowik, J. G., Bukowiecki, N., Prévôt, A. S. H., Baltensperger,
470 U., Schneider, J., Kimmel, J. R., Gonin, M., Rohner, U., Worsnop, D. R., and Jayne, J. T.:
471 The ToF-ACSM: a portable aerosol chemical speciation monitor with TOFMS detection,
472 Atmos Meas Tech, 6, 3225–3241, https://doi.org/10.5194/amt-6-3225-2013, 2013.
473 Gamelas, C. A., Canha, N., Vicente, A., Silva, A., Borges, S., Alves, C., Kertesz, Z., and
474 Almeida, S. M.: Source apportionment of PM2.5 before and after COVID-19 lockdown in an
475 urban-industrial area of the Lisbon metropolitan area, Portugal, Urban Clim, 49, 101446,
476 https://doi.org/10.1016/j.uclim.2023.101446, 2023.
477 Hu, R., Wang, S., Zheng, H., Zhao, B., Liang, C., Chang, X., Jiang, Y., Yin, R., Jiang, J., and
478 Hao, J.: Variations and Sources of Organic Aerosol in Winter Beijing under Markedly
479 Reduced Anthropogenic Activities During COVID-2019, Environ Sci Technol, 56, 6956–
480 6967, https://doi.org/10.1021/acs.est.1c05125, 2022.
481 IPCC: Climate Change 2021 – The Physical Science Basis, Cambridge University Press,
482 https://doi.org/10.1017/9781009157896, 2021.
483 Jayne, J. T., Leard, D. C., Zhang, X., Davidovits, P., Smith, K. A., Kolb, C. E., and Worsnop,
484 D. R.: Development of an Aerosol Mass Spectrometer for Size and Composition Analysis of
485 Submicron Particles, Aerosol Science and Technology, 33, 49–70,
486 https://doi.org/10.1080/027868200410840, 2000.
487 Jeong, C.-H., Yousif, M., and Evans, G. J.: Impact of the COVID-19 lockdown on the
488 chemical composition and sources of urban PM2.5, Environmental Pollution, 292, 118417,
489 https://doi.org/10.1016/j.envpol.2021.118417, 2022.
490 Jimenez, J. L., Canagaratna, M. R., Donahue, N. M., Prevot, A. S. H. H., Zhang, Q., Kroll, J.
491 H., DeCarlo, P. F., Allan, J. D., Coe, H., Ng, N. L., Aiken, A. C., Docherty, K. S., Ulbrich, I.

https://doi.org/10.5194/egusphere-2024-4041
Preprint. Discussion started: 14 January 2025

M., Grieshop, A. P., Robinson, A. L., Duplissy, J., Smith, J. D., Wilson, K. R., Lanz, V. A., Hueglin, C., Sun, Y. L., Tian, J., Laaksonen, A., Raatikainen, T., Rautiainen, J., Vaattovaara, P., Ehn, M., Kulmala, M., Tomlinson, J. M., Collins, D. R., Cubison, M. J., Dunlea, J., Huffman, J. A., Onasch, T. B., Alfarra, M. R., Williams, P. I., Bower, K., Kondo, Y., Schneider, J., Drewnick, F., Borrmann, S., Weimer, S., Demerjian, K., Salcedo, D., Cottrell, L., Griffin, R., Takami, A., Miyoshi, T., Hatakeyama, S., Shimono, A., Sun, J. Y., Zhang, Y. M., Dzepina, K., Kimmel, J. R., Sueper, D., Jayne, J. T., Herndon, S. C., Trimborn, A. M., Williams, L. R., Wood, E. C., Middlebrook, A. M., Kolb, C. E., Baltensperger, U., Worsnop, D. R., Dunlea, E. J., Huffman, J. A., Onasch, T. B., Alfarra, M. R., Williams, P. I., Bower, K., Kondo, Y., Schneider, J., Drewnick, F., Borrmann, S., Weimer, S., Demerjian, K., Salcedo, D., Cottrell, L., Griffin, R., Takami, A., Miyoshi, T., Hatakeyama, S., Shimono, A., Sun, J. Y., Zhang, Y. M., Dzepina, K., Kimmel, J. R., Sueper, D., Jayne, J. T., Herndon, S. C., Trimborn, A. M., Williams, L. R., Wood, E. C., Middlebrook, A. M., Kolb, C. E., Baltensperger, U., and Worsnop, D. R.: Evolution of Organic Aerosols in the Atmosphere, Science (1979), 326, 1525–1529, https://doi.org/10.1126/science.1180353, 2009.

Kelly, F. J. and Fussell, J. C.: Size, source and chemical composition as determinants of toxicity attributable to ambient particulate matter, Atmos Environ, 60, 504–526, https://doi.org/10.1016/j.atmosenv.2012.06.039, 2012.

Middlebrook, A. M., Bahreini, R., Jimenez, J. L., and Canagaratna, M. R.: Evaluation of Composition-Dependent Collection Efficiencies for the Aerodyne Aerosol Mass Spectrometer using Field Data, Aerosol Science and Technology, 46, 258–271, https://doi.org/10.1080/02786826.2011.620041, 2012.

https://doi.org/10.5194/egusphere-2024-4041
Preprint. Discussion started: 14 January 2025

514 Mohr, C., Huffman, J. A., Cubison, M. J., Aiken, A. C., Docherty, K. S., Kimmel, J. R.,
515 Ulbrich, I. M., Hannigan, M., and Jimenez, J. L.: Characterization of primary organic aerosol
516 emissions from meat cooking, trash burning, and motor vehicles with high-resolution aerosol
517 mass spectrometry and comparison with ambient and chamber observations, Environ Sci
518 Technol, 43, 2443–2449,
519 https://doi.org/10.1021/ES8011518/SUPPL_FILE/ES8011518_SI_001.PDF, 2009.
520 Ng, N. L., Herndon, S. C., Trimborn, A., Canagaratna, M. R., Croteau, P. L., Onasch, T. B.,
521 Sueper, D., Worsnop, D. R., Zhang, Q., Sun, Y. L., and Jayne, J. T.: An Aerosol Chemical
522 Speciation Monitor (ACSM) for Routine Monitoring of the Composition and Mass
523 Concentrations of Ambient Aerosol, Aerosol Science and Technology, 45, 780–794,
524 https://doi.org/10.1080/02786826.2011.560211, 2011a.
525 Ng, N. L., Canagaratna, M. R., Jimenez, J. L., Zhang, Q., Ulbrich, I. M., and Worsnop, D. R.:
526 Real-Time Methods for Estimating Organic Component Mass Concentrations from Aerosol
527 Mass Spectrometer Data, Environ Sci Technol, 45, 910–916,
528 https://doi.org/10.1021/es102951k, 2011b.
529 GDP and events in history: how the COVID-19 pandemic shocked the UK economy:
530 https://www.ons.gov.uk/economy/grossdomesticproductgdp/articles/gdpandeventsinhistory
531 howthecovid19pandemicshockedtheukeconomy/2022-05-24, last access: 26 November 2024.
532 Paatero, P.: The Multilinear Engine—A Table-Driven, Least Squares Program for Solving
533 Multilinear Problems, Including the n -Way Parallel Factor Analysis Model, Journal of
534 Computational and Graphical Statistics, 8, 854–888,
535 https://doi.org/10.1080/10618600.1999.10474853, 1999.

https://doi.org/10.5194/egusphere-2024-4041
Preprint. Discussion started: 14 January 2025

536 Paatero, P. and Hopke, P. K.: Rotational tools for factor analytic models, J Chemom, 23, 91–
537 100, https://doi.org/10.1002/cem.1197, 2009.
538 Paatero, P. and Tapper, U.: Positive matrix factorization: A non-negative factor model with
539 optimal utilization of error estimates of data values, Environmetrics, 5, 111–126,
540 https://doi.org/10.1002/env.3170050203, 1994.
541 Paatero, P., Hopke, P. K., Song, X.-H., and Ramadan, Z.: Understanding and controlling
542 rotations in factor analytic models, Chemometrics and Intelligent Laboratory Systems, 60,
543 253–264, https://doi.org/10.1016/S0169-7439(01)00200-3, 2002.
544 Parworth, C., Fast, J., Mei, F., Shippert, T., Sivaraman, C., Tilp, A., Watson, T., and Zhang,
545 Q.: Long-term measurements of submicrometer aerosol chemistry at the Southern Great
546 Plains (SGP) using an Aerosol Chemical Speciation Monitor (ACSM), Atmos Environ, 106,
547 43–55, https://doi.org/10.1016/j.atmosenv.2015.01.060, 2015.
548 Petit, J.-E., Dupont, J.-C., Favez, O., Gros, V., Zhang, Y., Sciare, J., Simon, L., Truong, F.,
549 Bonnaire, N., Amodeo, T., Vautard, R., and Haeffelin, M.: Response of atmospheric
550 composition to COVID-19 lockdown measures during spring in the Paris region (France),
551 Atmos Chem Phys, 21, 17167–17183, https://doi.org/10.5194/acp-21-17167-2021, 2021.
552 Seinfeld, J. H., Wiley, J., and Pandis, S. N.: ATMOSPHERIC From Air Pollution to Climate
553 Change SECOND EDITION, 628–674 pp., 2006.
554 Tian, J., Wang, Q., Zhang, Y., Yan, M., Liu, H., Zhang, N., Ran, W., and Cao, J.: Impacts of
555 primary emissions and secondary aerosol formation on air pollution in an urban area of China
556 during the COVID-19 lockdown, Environ Int, 150, 106426,
557 https://doi.org/10.1016/j.envint.2021.106426, 2021.

https://doi.org/10.5194/egusphere-2024-4041
Preprint. Discussion started: 14 January 2025

558 Tobler, A. K., Skiba, A., Wang, D. S., Croteau, P., Styszko, K., Nęcki, J., Baltensperger, U.,
559 Slowik, J. G., and Prévôt, A. S. H.: Improved chloride quantification in quadrupole aerosol
560 chemical speciation monitors (Q-ACSMs), Atmos Meas Tech, 13, 5293–5301,
561 https://doi.org/10.5194/amt-13-5293-2020, 2020.
562 Transport for London: Travel in London Report 13, 2020.
563 Via, M., Chen, G., Canonaco, F., Daellenbach, K. R., Chazeau, B., Chebaicheb, H., Jiang, J.,
564 Keernik, H., Lin, C., Marchand, N., Marin, C., O'dowd, C., Ovadnevaite, J., Petit, J.-E.,
565 Pikridas, M., Riffault, V., Sciare, J., Slowik, J. G., Simon, L., Vasilescu, J., Zhang, Y., Favez,
566 O., Prévôt, A. S. H., Alastuey, A., and Cruz Minguillón, M.: Rolling vs. seasonal PMF: Real-
567 world multi-site and synthetic dataset comparison, Atmos Meas Tech, 15,
568 https://doi.org/10.5194/amt-15-5479-2022, 2022.
569 Wei, Y., Qiu, X., Yazdi, M. D., Shtein, A., Shi, L., Yang, J., Peralta, A. A., Coull, B. A., and
570 Schwartz, J. D.: The Impact of Exposure Measurement Error on the Estimated Concentration–
571 Response Relationship between Long-Term Exposure to PM2.5 and Mortality, Environ
572 Health Perspect, 130, https://doi.org/10.1289/EHP10389, 2022.
573 Wei, Y., Feng, Y., Danesh Yazdi, M., Yin, K., Castro, E., Shtein, A., Qiu, X., Peralta, A. A.,
574 Coull, B. A., Dominici, F., and Schwartz, J. D.: Exposure-response associations between
575 chronic exposure to fine particulate matter and risks of hospital admission for major
576 cardiovascular diseases: population based cohort study, BMJ, e076939,
577 https://doi.org/10.1136/bmj-2023-076939, 2024.
578 World Health Organization: WHO global air quality guidelines. Particulate matter (PM2.5
579 and PM10), ozone, nitrogen dioxide, sulfur dioxide and carbon monoxide., Geneva, 2021.

https://doi.org/10.5194/egusphere-2024-4041
Preprint. Discussion started: 14 January 2025

580 Xu, J., Ge, X., Zhang, X., Zhao, W., Zhang, R., and Zhang, Y.: COVID-19 Impact on the
581 Concentration and Composition of Submicron Particulate Matter in a Typical City of
582 Northwest China, Geophys Res Lett, 47, https://doi.org/10.1029/2020GL089035, 2020.
583 Zhang, Q., Jimenez, J. L., Canagaratna, M. R., Ulbrich, I. M., Ng, N. L., Worsnop, D. R., and
584 Sun, Y.: Understanding atmospheric organic aerosols via factor analysis of aerosol mass
585 spectrometry: a review, Anal Bioanal Chem, 401, 3045–3067,
586 https://doi.org/10.1007/s00216-011-5355-y, 2011.
587
588